Journal of Computer-Aided Molecular Design, 10 (1996) 107–122
ESCOM

J-CAMD 334

On the electrostatic and steric similarity of lactam compounds and the natural substrate for bacterial cell-wall biosynthesis

J. Frau* and S.L. Price

Department of Chemistry, University College London, London WC1H 0AJ, U.K.

Received 26 June 1995
Accepted 26 December 1995

Keywords: Electrostatic similarity; Molecular electrostatic potential; β-Lactam compounds; γ-Lactam compounds; Distributed multipoles

Summary

Electrostatic and structural properties of a set of β-lactam, γ-lactam and nonlactam compounds have been analyzed and compared with those of a model of the natural substrate D-alanyl-D-alanine for the carboxy- and transpeptidase enzymes. This first comparison of the electrostatic properties has been based on a distributed multipole analysis of high-quality ab initio wave functions of the substrate and potential antibiotics. The electrostatic similarity of the substrate and active compounds is apparent, and contrasts with the electrostatic properties of the noninhibitors. This has been quantified to give a reasonable correlation with the MIC (Minimum Concentration for Inhibition) and with kinetic data (k_2/K) in accordance with the model for interaction of the lactam compounds with DD-peptidase. These correlations provide a better prediction of antibacterial activity than purely structural criteria.

Introduction

The biosynthesis of bacterial cell-wall peptidoglycan is catalyzed and controlled in its final stages by carboxy- and transpeptidase enzymes, which act on the D-alanyl-D-alanine peptide appendages of *N*-acetylmuramyl-*N*-acetyl-glucosyl polysaccharides [1,2]. In 1965 Tipper and Strominger [3] proposed that β-lactam antibiotics act as inhibitors of the transpeptidase enzyme, because they mimic the active conformation of the terminal D-alanyl-D-alanine. Further studies by Lee [4] pointed out that the conformation of penicillin is most similar to that of D-Ala-D-Ala if the dihedral angle around the peptide bond in D-Ala-D-Ala is distorted by approximately 45°.

The interaction of DD-peptidases with D-Ala-D-Ala substrate and β-lactams is described by a three-step mechanism in which enzyme and substrate first react to form the noncovalent complex. In the second step, a covalently bound acyl–enzyme intermediate forms, which reacts further into the products. β-Lactams that are effective active-site inhibitors of cell-wall biosynthesis require: (a) sufficient structural and electrostatic similarity with physiological substrates to permit recognition by essential cell-wall enzymes; and (b) a highly reactive β-lactam bond to facilitate rapid acylation of the enzyme's active site [5–7]. Since the initial recognition is likely to be dominated by electrostatic forces, the antibiotics and the substrate, which bind to the same receptor site in the peptidase enzyme, would be expected to have similar electrostatic properties. Thus, we present the first comparison of the electrostatic properties of the lactam compounds, applying the emerging philosophy in drug design that molecules with similar patterns in the electrostatic potential outside their van der Waals surfaces may well bind to the same receptor [8–17]. Given the range of functional groups found in the antibiotics, it is essential that realistic models are used for the electrostatic forces. In this work, the charge distribution around each atom is represented by a charge, dipole, quadrupole, etc., derived by a Distributed Multipole Analysis (DMA) [18] of a high-quality ab initio wave function of the molecule. The higher multipole moments represent the nonspherical features in the valence electron distribution around each atom, such as lone pairs and π-electrons. Such nonspherical features are often invoked in rationalizing organic reaction mechanisms and hydrogen-bonding geometries. Previous studies of the

*To whom correspondence should be addressed at: Departament de Quimica-Fisica, Edifici Mateu Orfila i Rotger, Universitat de les Illes Balears, E-07071 Palma de Mallorca, Spain.

phosphodiesterase III substrate and its inhibitors [19] and of adenosine receptor ligands [20] have shown that the electrostatic similarity between ligands that bind to the same site is more apparent if these accurate electrostatic models are used rather than approximate atomic charges.

The aim of this work is to study the structural and electrostatic similarities between the natural substrate of the carboxy enzymes and transpeptidases, the transition state of this structure and the lactam antibiotic inhibitors of these enzymes, seeking characteristics that distinguish between known inhibitors and superficially similar lactam noninhibitors. These electrostatic similarities are very important in the initial recognition and binding of the antibiotic before covalent bond formation. The comparison of the structural and electrostatic properties of these compounds, with possible bound conformations of the substrate, allows determination of the characteristics necessary for inhibitory activity.

The substrate D-alanyl-D-alanine appendage is modelled by *N*-acetyl-D-alanyl-D-alanine, the conformation of which is determined by six dihedral angles (Fig. 1). A wide range (Fig. 2) of structurally and chemically diverse inhibitors, and some related noninhibitors were studied. These include some important β-lactam inhibitors (ampicillin (**1**), a penicillin with an equatorial conformation of the thiazolidine ring, cephalotin (**3**), one oxacephem (**4**), and one monobactam (**5**)) and poor inhibitors (penicillin V (**2**), with an axial conformation of the thiazolidine ring, and two Δ^2-cephem isomers (**8** and **9**)), two compounds resistant to β-lactamases (imipenem (**6**), which resists β-lactamase hydrolysis and is a very good antibiotic, and clavulanic acid (**7**), one of the most important inhibitors for β-lactamases and a really poor antibiotic), two β-lactam structures (pyrazolidinone (LY186826) (**10**), and the noninhibitor γ-lactam azetidine (**11**)), and finally two nonlactam structures: lactivicin (*S* (**12**) and *R* (**13**)), and the noninhibitor deazacarbapenam (**14**). For the structures **1**, **2**, **3** and **10** the extensive C_6 or C_7 side chain has been replaced by an acetamide group to facilitate the ab initio calculations.

Methods

Determination of plausible bound conformations of the D-Ala-D-Ala subunit

A variety of different conformations of D-Ala-D-Ala have been generated in order to find a suitable model. One obviously low-energy conformation is the crystal structure of phenylacetyl-D-alanyl-D-alanine (CSD code: DIFNAH) [21] in which the phenyl group in the side chain was replaced by a methyl group in order to compare this structure with penicillins and cephalosporins. This was used as a starting point in a conformational analysis, using the CVFF [22] molecular mechanics force field with the Newton-Raphson algorithm in the Insight II [23] software, running on a Silicon Graphics workstation. The complete conformational space of the torsion angles $\phi_2,\psi_2,\phi_3,\psi_3$, was searched in 30° steps, with the minima being refined to within 5°. All of these constrained minima were then completely optimized.

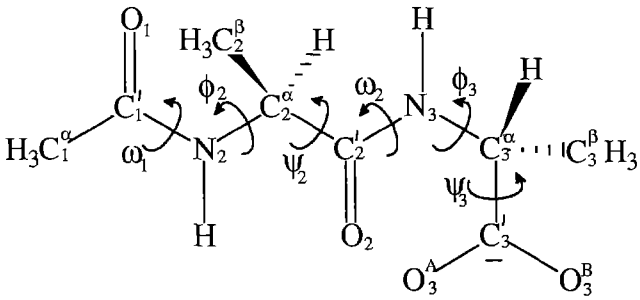

Fig. 1. *N*-Acetyl-D-alanyl-D-alanine in the extended conformation, showing the notation used for the atoms and dihedral angles.

The complete energy minimisations show several plausible low-energy structures (Table 1). The minima M2 and M3 have ϕ,ψ dihedral angles characteristic of a β-pleated sheet and a right-handed α-helix, respectively. As can be seen, some of these minina show an ω_2 dihedral angle that differs significantly from the 180° found in most of the crystallographic structures of the oligopeptide crystals accumulated in the Cambridge Structural Database (CSD) [24]. Nevertheless, although the prediction of larger deviations from planarity at the nitrogen atom may imply that such distortions could be quite accessible in the gas phase or in a binding site, these could be an artefact of the potential parameterisation.

We also produced two model structures by manually adjusting the ϕ,ψ torsion angles to resemble the orientation of the side chains (up to the acetamide group) in the crystal structures of ampicillin (SAP) [25] and cephalotin (SCP) [26], using the bond lengths, bond angles and ω_1 and ω_2 dihedral angles of the substrate crystal structure.

For comparison, we also included structures with torsion angles determined by other methods to obtain energy minima for model substrates. SC1 and SC2 are the most stable structures obtained by De Coen et al. [27] in a conformational analysis of Ac-L-Lys-D-Ala-D-Ala and very close to the structures obtained by Virudachalam and Rao [28]. A rather different minimum (SN) obtained by Neuhaus and Hammes [29], using the molecular mechanics method, is also included.

Previous studies pointed out that β-lactam antibiotics show conformations similar to the deformed conformation of the D-Ala-D-Ala portion of the natural substrate, postulated to be the transition state during cleavage or formation of a peptide bond, and the peptidoglycan transpeptidase is presumed to bind preferentially to such a distorted D-Ala-D-Ala geometry that closely resembles that of the penicillins [4,30]. According to this modified model, enzyme action on the natural substrate should

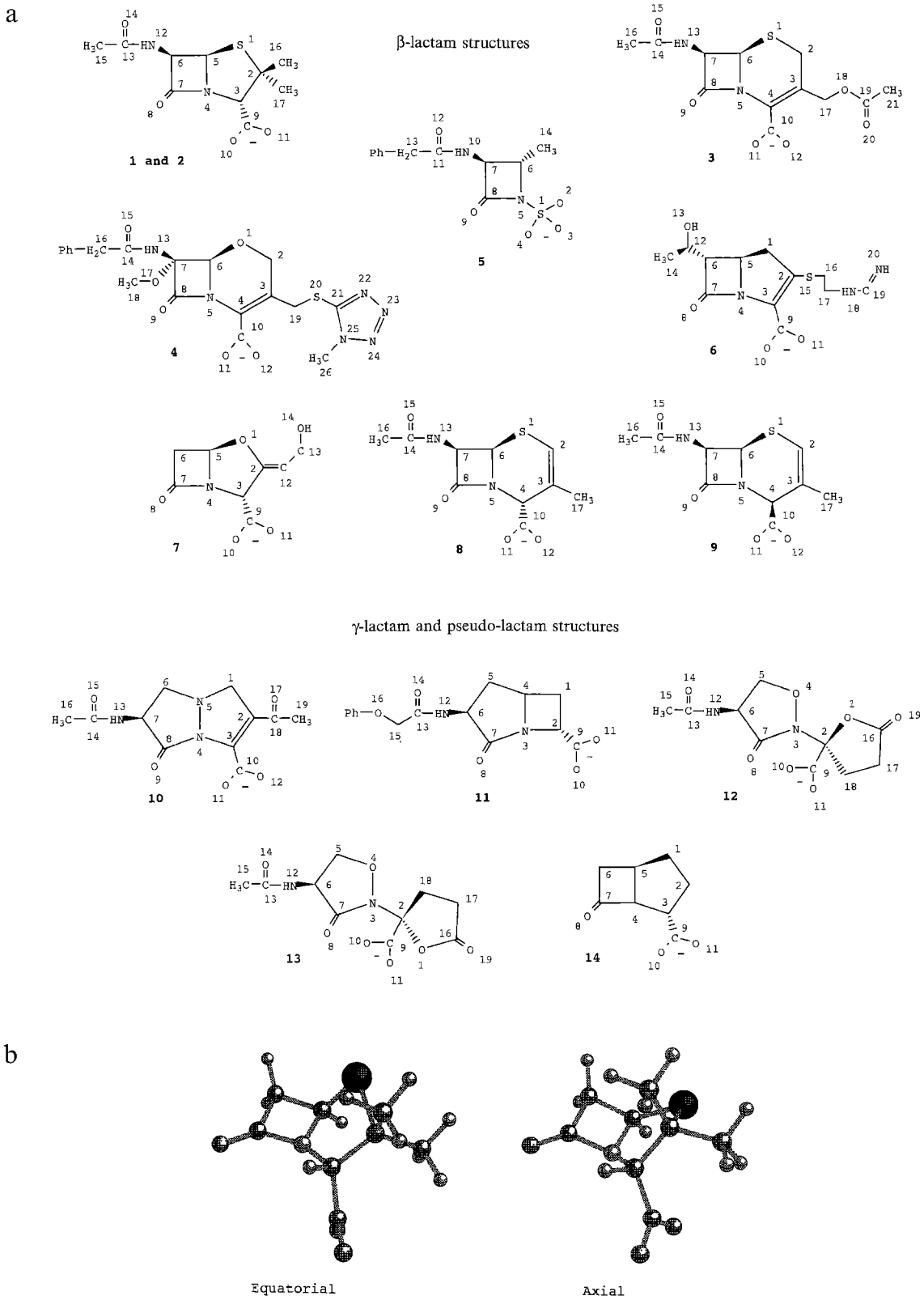

Fig. 2. (a) Set of β-lactam, γ-lactam and nonlactam structures and the notation used for the nonhydrogen atoms. β-Lactam compounds: 'ampicillin' (**1**), 'penicillin V' (**2**), 'cephalotin' (**3**), oxacephem (**4**), monobactam (**5**), imipenem (**6**), clavulanic acid (**7**), Δ^2-cephem-4α-carboxylic acid (**8**) and Δ^2-cephem-4β-carboxylic acid (**9**); γ-lactam structures: pyrazolidinone (**10**) and γ-lactam azetidine (**11**); and nonlactam structures: (*S*)-lactivicin (**12**), (*R*)-lactivicin (**13**) and deaza-carbapenam (**14**). Structures **1**, **2**, **3** and **10** are models obtained from ampicillin, penicillin V, cephalotin and bicyclic pyrazolidinone LY186826, by changing the side chain at C_6 or C_7 for a CH_3-CO-NH group. Structures **8**, **9**, **10** and **14** have been modelled and optimised with the Insight II software; the other structures have been obtained from the Cambridge Structural Database. (b) Equatorial (**1**) and axial (**2**) conformations of the thiazolidine ring of penicillins.

TABLE 1
VALUES OF RELATIVE CVFF CONFORMATIONAL ENERGIES FOR VARIOUS CONFORMATIONS OF THE *N*-ACETYL-D-ALANYL-D-ALANINE SUBSTRATE

	E (kJ mol^{-1})	ω_1 (°)	ϕ_2 (°)	ψ_2 (°)	ω_2 (°)	ϕ_3 (°)	ψ_3 (°)
Crystal	64.8	177.6	98.4	−154.7	178.0	61.5	30.8
SAP[a]	38.1	177.6	144.7	−127.8	178.0	78.7	16.8
SCP[a]	128.0	177.6	149.8	−93.0	178.0	36.6	40.0
M1	0.0	−176.2	143.6	62.8	−169.1	140.7	45.0
M2	2.5	−177.0	144.5	−138.6	−173.0	144.2	46.7
M3	30.1	173.6	−65.9	−69.6	−172.4	148.2	46.6
M4	31.0	−168.9	142.7	−63.3	131.4	−92.4	52.2
M5	35.1	165.7	−83.8	44.2	−157.6	107.8	40.2
M6	64.0	165.1	−83.0	−72.6	122.6	−115.1	48.7
M7	71.1	175.7	−72.6	81.1	159.0	−85.5	68.1
SC1[b]	58.2	−179.9	80.0	−80.0	180.0	160.0	20.0
SC2[b]	34.7	−179.9	160.0	−160.0	180.0	160.0	20.0
SN[b]	44.3	−179.9	180.0	−125.0	180.0	150.0	30.0
TS[c]	107.9	−179.9	145.0	−120.0	135.0	80.0	30.0

The hydrogen atoms in the structures derived from the crystal structure of phenylacetyl-D-alanyl-D-alanine have been added to carbon and nitrogen atoms with the standard bond lengths of 1.08 Å and 1.01 Å [49], respectively. In these structures the carboxylate form has been used with standard bond lengths (1.25 Å) [49].

[a] Bond lengths, bond angles and ω_1 and ω_2 dihedral angles were obtained from the crystal structure.

[b] Bond lengths and bond angles were obtained from the global minimum.

[c] Bond lengths and bond angles were obtained from the global minimum. Parameters directly involved in the twisting of the C-N bond were obtained from AM1 calculations. Dihedral angles were determined by steric fitting into DD-peptidase [31].

involve the distortion of the D-Ala-D-Ala peptide bond to a pyramidal shape. Kelly et al. [31] pointed out that it is quite conceivable that the serine hydroxyl, as it attacks the anchored peptide, would approach the C-terminal C-N bond close enough to cause such a rotation out of planarity. This enzymatic distortion of X-D-Ala-D-Ala towards the TS conformation proposed for β-lactam inhibitors generates a site-constrained conformation (TS), which fits into DD-peptidase from *Streptomyces* R61. The significance of such an internal rotation may be that the transition state in the transpeptidation process more nearly has this conformation [32]. Such a conformational change has the effect of activating the peptide bond toward nucleophilic attack, such as in hydrolysis or acylation. A distortion that weakens the C-N bond and in which the amide nitrogen is tetrahedrally hybridized seems likely to occur in the formation of the TS, because this bond is broken in the final cross-linking of the peptidoglycan chains [33]. Table 1 suggests that the energy required to distort the substrate to a penicillin-like transition-state conformation is sufficiently low that it could be derived by the stabilizations achieved by the interaction of the enzyme and substrate at the receptor site.

Structural overlay of substrate conformations and transition state with β-lactams

We now quantify the structural similarity between the different conformations of the substrate and the crystal-structure conformations of ampicillin and cephalotin, to determine the most plausible active conformations. Each substrate conformation was overlaid on each ligand molecule by minimising the root-mean-square (rms) distances between specified pairs of atoms that are expected to be in the same position in the active site, using the 3D molecular graphics software Insight II [23].

It is debatable how much of the peptide chain must be structurally similar to the antibiotic ligands. The overlapping sequence has to include: the carbonyl group (C'_2 and O_2 atoms), since this group represents the reaction center if the substrate or antibiotic is bound to the cell-wall enzymes; the carboxylic group (C'_3), believed [34] to be essential for antibacterial activity; and the amide group in the side chain (N_2), which is necessary in normal penicillins and cephalosporins. However, some β-lactam structures (e.g. imipenem (**6**)) without an acylamino side chain possess significant antibacterial activity.

Hence we considered a variety of overlay sequences (Table 2), for those conformations in Table 1 that were plausible candidates for resembling the active conformation of the substrate. The best structural overlays with either ampicillin or cephalotin are obtained with the SAP structure and obviously with the TS structure (Figs. 3 and 4). The best fit around the nonplanar nitrogen of ampicillin and cephalotin is obtained with the TS structure. However, Table 2 reveals that this nonplanar structure does not produce a significantly better fit in the bulkier regions: the rms values for the various overlays are similar to those obtained with the SAP structure, which has a planar nitrogen atom.

Our analysis suggests that a comparable structural similarity between the substrate and antibiotic ligands can be obtained with either a planar or a pyramidal nitrogen.

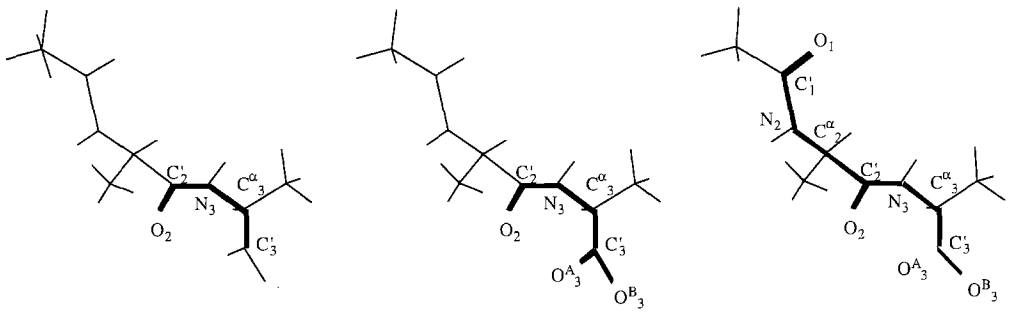

Scheme 1. From left to right: overlays 1, 2 and 3 (Table 2) between various conformations of the substrate with ampicillin and cephalotin.

However, structural similarity is not the only determinant of the ability to bind in the same site, and within the range of structures that can sterically fit, the electrostatic similarity is likely to be more important than the finer details of steric overlap. Thus, in order to compare the electrostatic properties of ligands and the substrate, two model substrates were used, namely SAP and TS. These represent two acceptable steric fits, differing most significantly in having a planar and a pyramidal nitrogen, respectively, as well as in their bond lengths and bonds angles, especially those related to the peptidic bond. The use of the two models for the substrate provides some indication for the sensitivity of the recognition to the substrate structure.

Electrostatic similarity

Methodology

The geometries of the β-lactam, γ-lactam and nonlactam structures in Fig. 2a were obtained from crystallographic data, using the CSD, or where necessary were determined by energy optimization with the CVFF molecular mechanics force field using Insight II. The main problem is defining the conformation of the amino-acyl side chains on the penicillin, cephalosporin or γ-lactam skeletons, since this seems to have an influence on antibacterial activity and β-lactamase resistance of these compounds [35,36]. The C_{13}-N_{12}-C_6-C_7 dihedral angle varies from 90° to 175° in crystal structures of penicillins. We have assumed a value of 165°, which is in the range of 160°–180° obtained in MM2 calculations of the most stable conformer [37]. A similar value of 165° has been used for the corresponding C_{11}-N_{10}-C_7-C_8 dihedral angle in monobactam. Most of the cephalosporins adopt a similar orientation for the 7-amino acyl side chain, with C_{14}-N_{13}-C_7-C_8 dihedral angles ranging from 130° to 180° in their crystal structures. We have used the crystallographic values, which are close to 170°, in cephalotin and oxacephem. The γ-lactam and nonlactam structures generated by energy minimisation have C_{13}-N_{12}-C_6-C_7 (C_{14}-N_{13}-C_7-C_8 in pyrazolidinone) dihedral angles close to 175° [37].

The electrostatic models were derived from the SCF wave function of each molecule, calculated with a 3-21G [38] basis set using the CADPAC [39] ab initio program suite. This basis set is expected to give the calculated potential minima in essentially the same positions as more accurate wave functions. A detailed study of the DMA-generated electrostatic potential around the alanine dipeptide ($CH_3CONHCHCH_3CONHCH_3$) showed it varied within a scaling factor with basis set and electron correlation for the 3-21G and larger basis sets [40]. Each wave function was represented by sets of multipoles up to the hexadecapole at each atomic site, obtained by a DMA [18]. The electrostatic potential was calculated from

TABLE 2
STRUCTURAL OVERLAYS OF VARIOUS CONFORMATIONS OF THE SUBSTRATE WITH AMPICILLIN AND CEPHALOTIN

Substituent conformation	Overlay 1		Overlay 2		Overlay 3	
	Ampicillin	Cephalotin	Ampicillin	Cephalotin	Ampicillin	Cephalotin
Crystal	0.35	0.22	0.40	0.22	0.87	0.71
SAP	0.24	0.26	0.28	0.28	0.52	0.44
SCP	0.48	0.25	0.57	0.25	0.59	0.31
M2	0.36	0.63	0.60	0.90	0.81	0.97
M1	0.36	0.63	0.59	0.88	1.29	1.56
SC1	0.43	0.69	0.56	0.89	1.19	1.41
SC2	0.43	0.69	0.56	0.89	0.72	0.91
SN	0.37	0.64	0.53	0.85	0.64	0.90
TS	0.26	0.15	0.33	0.17	0.51	0.41

Rms distances (Å) between the atoms specifying the overlay (see Scheme 1) and the corresponding atoms of the O_{14},C_{13},N_{12},C_6,C_7,O_8,N_4,C_5,C_9,O_{10}, O_{11} sequence of ampicillin or the O_{15},C_{14},N_{13},C_7,C_8,O_9,N_5,C_4,C_{10},O_{11},O_{12} sequence of cephalotin, in their respective crystal structure conformations.

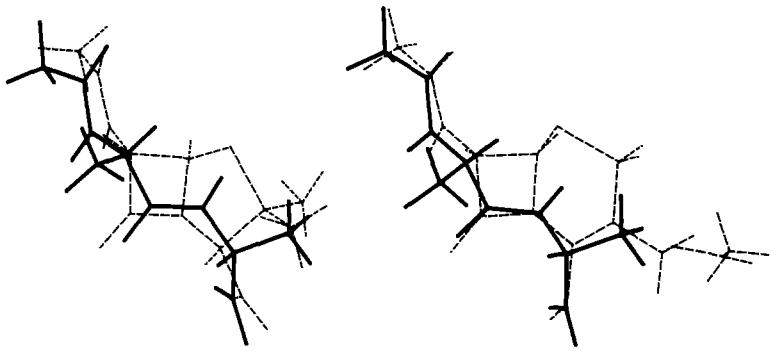

Fig. 3. Structural overlays (overlay 3, Table 2) obtained between the SAP (bold line) substrate and ampicillin (left), and cephalotin (right), respectively.

DMAs, using all terms in the multipole expansion up to R^{-5}, within the program ORIENT [41]. This procedure is expected to give the electrostatic potential, excluding the effects of penetration within the charge distribution, to essentially the accuracy of the wave function.

The electrostatic potential was examined at fixed distances outside the van der Waals surfaces of the molecules, as defined by the Pauling radii: 1.5 Å for N; 1.4 Å for O; 2 Å for CH (united atom); and 1.85 Å for S. There was no explicit hydrogen van der Waals radius, since the hydrogen atom is included in a united atom methyl radius, and polar hydrogen atoms effectively have no radius if involved in hydrogen bonding. Visual comparisons (Figs. 5–7) were made using a grid of points 1.4 Å from the van der Waals surface, approximating the water-accessible surface of the molecule. This is as close as any atom is likely to approach the molecule, except hydrogen-bonding protons and some small ions, and therefore it is a useful surface for visualising the electrostatic forces involved in general van der Waals contacts.

In addition to the visual comparison, a quantitative comparison of electrostatic similarity can be made using the positions of the extrema of the electrostatic potential at fixed distances from the molecules. The alignment of extrema of the same sign and similar magnitude between a ligand and substrate ensures a similar electrostatic potential around the two molecules in the matched regions. Since the electrostatic extrema correspond to regions where strong interactions such as hydrogen bonds with the binding site are possible, some of the extrema of the ligand and substrate are expected to overlay (to within approximately 1 Å) if they correspond to important van der Waals contacts between the ligands and binding site. It has been observed that there is a good overlay of the electrostatic extrema of phosphodiesterase III inhibitors and those of the substrate, in plausible relative binding orientations [19]. In the case of the transpeptidase enzyme, the substrate and inhibitors are negatively charged at physiological pH, and so we only consider the positions and strengths of the minima in the electrostatic potential energy, at the distance that would be sampled by a hydrogen-bonding proton of the binding site. These were determined by minimising the interaction energy of a single positive point charge (radius 0.5 Å) with each molecule, using pseudo hard-sphere repulsion between sites with nonzero van der Waals radii. We compared the electrostatic potential around these structures with that of the natural substrate D-Ala-D-Ala. For each molecule, a variety of superpositions relative to D-Ala-D-Ala were attempted, involving different combinations of minima. These were assessed by eye, and through the use of the minimised rms separations of the positions of the minima to the substrate and ligand.

Electrostatic modelling results

Electrostatic characteristics of the substrate models

The electrostatic potential around *N*-acetyl-D-alanyl-D-alanine is dependent on the conformation of the peptide. The potential on the water-accessible surface of the SAP structure (1.4 Å beyond the van der Waals surface) varies from −457 to −114 kJ mol^{-1}, which is similar to the range of −472 to −118 kJ mol^{-1} for the TS structure. Both potentials show a fairly smooth progression from the maximum around the region close to the methyl group (C_1^{α}) to the minimum near the carboxylate group. However, the pyramidality of N_3 in TS results in a less negative electrostatic potential around the C_2^{β} atom and a more negative potential in the carbonyl and peptidic region (O_2, $C_2^{\prime}$ and N_3) (Fig. 5).

Four distinct electrostatic minima occur in the electrostatic potential 0.5 Å from the SAP conformation of the substrate (Table 3). The deepest negative electrostatic potential region occurs near the carboxylate group with two minima in contact with O_3^A and O_3^B, respectively; however, there is another significant minimum near the carbonyl oxygen O_2. The final minimum near the carbonyl oxygen of the side chain (O_1) is much less deep. The loss of planarity of N_3 in the TS structure produces an additional weak minimum, presumably arising from the lone pair on this nitrogen atom, which is more delocalised in the planar amide group of the SAP structure.

However, this is the least negative of all minima and the other ones are analogous in location and energy to the minima obtained in the planar amide structure SAP. This picture of the electrostatic potential around the substrate is complementary to the description of the R61 DD-peptidase binding site by Kelly et al. [31], since the minima are related to the expected positions of hydrogen-bonding protons of the enzyme.

Lactam compounds and overlays

The electrostatic potential surfaces of the substrate conformations and the compounds were compared both visually and for the possibility of there being a sterically plausible overlay of the potential ligand and substrate, which overlaid the potential minima that are important in binding. The electrostatic overlays reported in Table 3 correspond to the smallest rms separations of minima around the substrate with the same four minima near to the oxygen atoms in the carboxylic and carbonyl groups in the lactam compounds.

*Penicillin: 'ampicillin' (equatorial; **1**) and 'penicillin V' (axial; **2**)* The electrostatic potential around the charged ampicillin varies from −425 to −114 kJ mol^{-1} and is very similar to the electrostatic potential around the substrate (Fig. 5), the most important difference being the negative electrostatic region above the sulphur atom. Apart from the four most important minima, there are two fairly shallow (−306.1 and −272.4 kJ mol^{-1}) minima in the sulphur atom region, as well as a minimum in the α-face related to the β-lactam nitrogen and one of the oxygen atoms in the carboxylic group. The most important difference between the crystal structures of ampicillin and penicillin V is that the conformation of the thiazolidine ring is equatorial in the first structure and axial in the second one (Fig. 2b), thus changing the orientation of the carboxylic group relative to the lactam ring and the electrostatic properties considerably (Fig. 6). The minima related to the sulphur and nitrogen atoms disappear and the location of the minima related to the carboxylic group is quite different. This is in accord with the evidence that the equatorial conformer of penicillins is mainly responsible for biological activity [42,43].

*Cephalosporin: 'cephalotin' (**3**)* The electrostatic potential around the charged cephalotin varies from −463 to −109 kJ mol^{-1}, and is in general similar to that of the substrate and ampicillin (Fig. 5). However, there is a very positive area around the methyl group in C_{21}, which extends beyond the former compounds. There are additional minima near the sulphur atom and the double bond of the dihydrothiazine ring, as well as related to the O_{18} atom. It is known that very long and wide substituents at the 3-position are accommodated in the target receptors. These larger substituents are usually connected to the cephem through two or more conformationally flexible bonds and can turn upwards out of the way when the cephalosporin is making its approach into the active site [44]. None of the extrema related to this chain overlay with minima of the substrate, but they could assist the binding of the cephalotin by interacting with parts of the enzyme that are not reached by the substrate.

*Oxacephem (**4**)* Replacement of the sulphur in the bicyclic ring structure by oxygen results in increased antibacterial activity against gram-negative bacteria [45]. The electrostatic potential on the accessible surface varies from −438 to −84 kJ mol^{-1} and again we can notice two regions with the highest potential values located at the ends of the C_3 and C_7 side chains and a gradual decrease of the electrostatic potential in the regions between these extrema. The minimum associated with the O_{15} atom is deepened by the proximity of O_{17}.

*Monobactam (**5**)* The most important structural characteristics of this compound are the replacement of the carboxylic group by a sulphonate group, the lack of a ring fused to the β-lactam ring and the resulting planarity of the β-lactam nitrogen. The electrostatic potential around this molecule varies from −427 to −89 kJ mol^{-1}, which is roughly similar to that of the substrate, but now the surface is dominated by the peptidic sequence and there is a wider negative region around the sulphonate group, since there is no chemical group to counteract it. Only three pairs of minima have been used in the electrostatic matching, although the fourth minimum of the substrate, near O_3^B, is still in a very negative potential region.

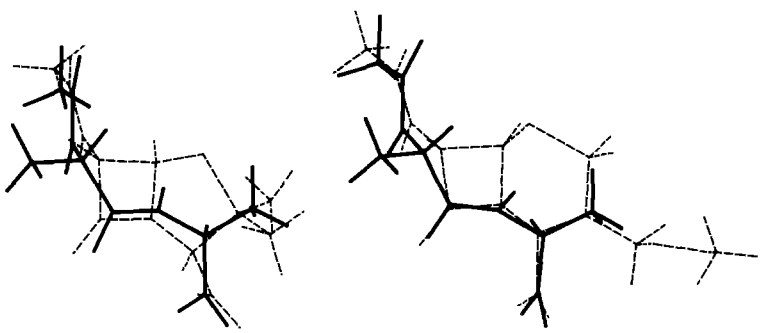

Fig. 4. Structural overlays (overlay 3, Table 2) obtained between the TS (bold line) substrate and ampicillin (left), and cephalotin (right), respectively.

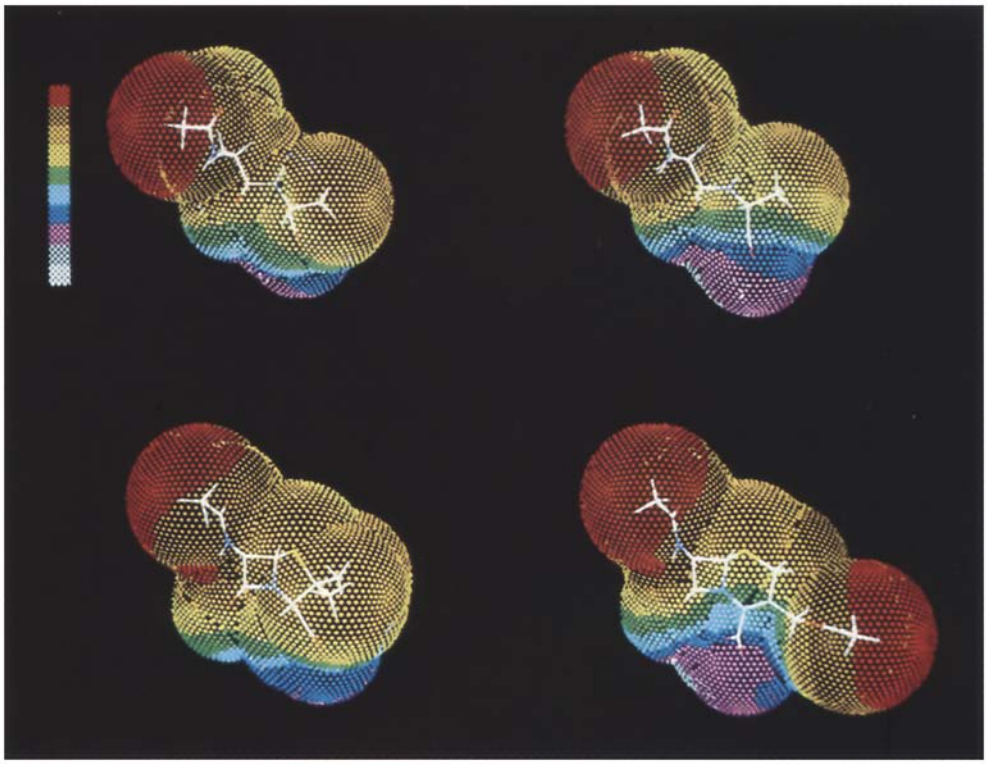

Fig. 5. A comparison of the electrostatic potential V (kJ mol^{-1}) on the water-accessible surface around the *N*-acetyl-D-alanyl-D-alanine substrate in the SAP conformation (top left) and the TS conformation (top right), and two active antibiotics: 'ampicillin', equatorial conformation (bottom left), and 'cephalotin' (bottom right). Colour code: white < −460 < grey < −420 < magenta < −380 < blue < −340 < cyan < −300 < green < −260 < yellow < −220 < orange < −180 < brown < −140 < red.

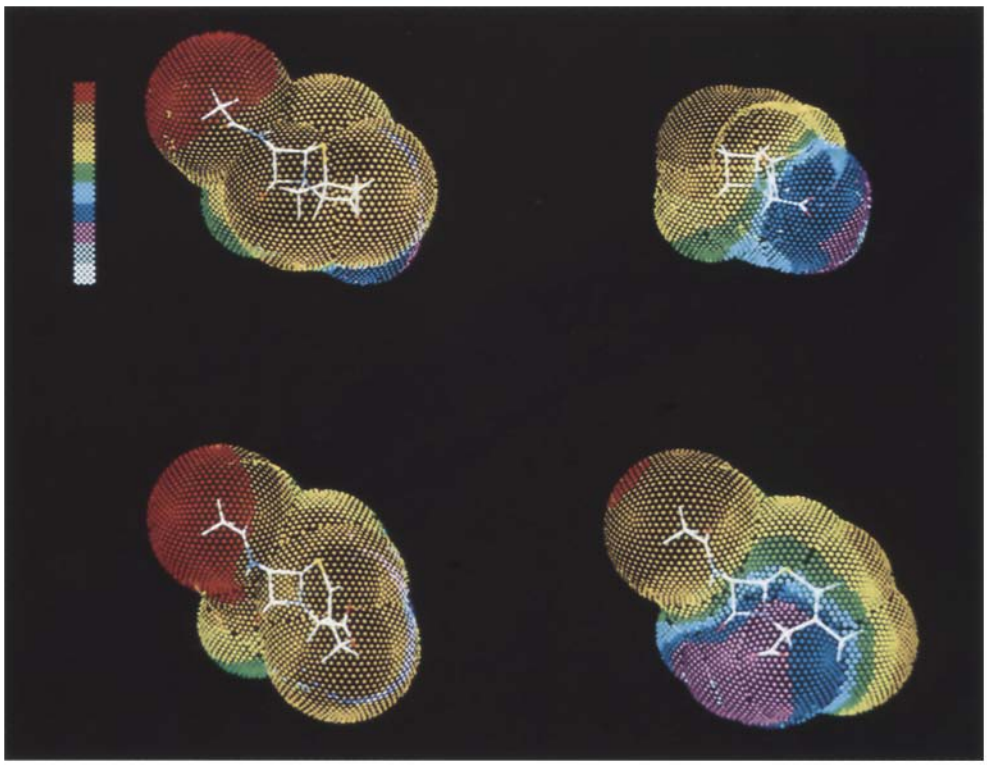

Fig. 6. The electrostatic potential V (kJ mol^{-1}) on the water-accessible surface around some noninhibitors: 'penicillin V', axial conformation (top left), clavulanic acid (top right), Δ^2-cephem-4α-carboxylic acid (bottom left) and Δ^2-cephem-4β-carboxylic acid (bottom right). Colour code: white < −460 < grey < −420 < magenta < −380 < blue < −340 < cyan < −300 < green < −260 < yellow < −220 < orange < −180 < brown < −140 < red.

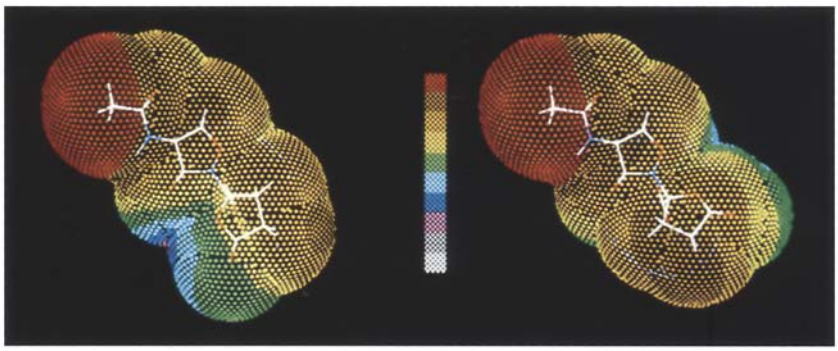

Fig. 7. The electrostatic potential V (kJ mol^{-1}) on the water-accessible surface around (*S*)-lactivicin (left) and (*R*)-lactivicin (right). Colour code: white < −460 < grey < −420 < magenta < −380 < blue < −340 < cyan < −300 < green < −260 < yellow < −220 < orange < −180 < brown < −140 < red.

Imipenem (6) Imipenem is one of the most important carbapenems due to its broad-spectrum activity and its resistance to β-lactamases. The water-accessible electrostatic potential surface of imipenem ranges from −462 to −54 kJ mol^{-1}, with the α-face being much more negative than the β-face. This antibiotic is unusual in that it does not have a 7β-amino-acyl side chain, which may account for its broad antibacterial spectrum [45]. However, the substrate electrostatic minima in this region can still be matched by the minima close to the oxygen atom of the hydroxyl group on the C_6 side chain. Indeed, the electrostatic overlays with the two model substrates are amongst the best obtained.

Clavulanic acid (7) Clavulanic acid belongs to the class of mechanism-based inhibitors of β-lactamases, sometimes referred to as suicide substrates, although the antibacterial activity of this compound by itself is very limited [46]. The electrostatic potential, which varies from −445 to −143 kJ mol^{-1} on the water-accessible surface, is rather different from that of the penicillins and cephalosporins. This is because the spatial location of the carboxylate group is constrained by the C_2=C_{12} bond, which makes it rather different. There is a very negative area close to the fused ring, but the minima associated with the carboxylate group are displaced sufficiently to give a poor electrostatic overlay with the substrates.

Δ^2-cephem isomers and other compounds The compounds 7β(acetylamino)-Δ^2-cephem-4α-carboxylic acid (**8**), 7β(acetylamino)-Δ^2-cephem-4β-carboxylic acid (**9**), γ-lactam azetidine (**11**) and deazacarbapenam (**14**) are structurally sufficiently similar to the active compounds in Fig. 2 that they should be tested for antibacterial activity, but none of them turned out to be active. There are more obvious differences between their electrostatic potential surfaces (Fig. 6) than between the structures. Table 3 shows the minima obtained in the electrostatic potential. In all cases the electrostatic fits with the model substrates are worse than those obtained with the inhibitor compounds.

Pyrazolidinone (10) Bicyclic pyrazolidinone, LY-186826, is the lead of a new class of synthetic γ-lactams, which exhibits broad-spectrum antibacterial activity against a variety of clinically important pathogens. The electrostatic potential ranges from −433 to −103 kJ mol^{-1} and the electrostatic surface obtained is very similar to the substrate surface. Despite the presence of the five-membered ring, we have found the same four main minima, and other minima related to the side chain (O_{17}) and to the nitrogen atoms in the γ-lactam system.

(S) epimer (12) and (R) epimer (13) of lactivicin This compound, which in solution is a mixture of the two C_2 epimers, shows a moderate antibacterial activity (MIC = 83.3, as defined in Table 3), with a very similar mode of action to that of β-lactam antibiotics [47]. A conformational analysis of the orientations of the rings with the CVFF force field predicts that both epimers have two minima, with similar energies. We only report the electrostatic overlay for the conformer of each epimer in which the carboxylic group is suitably oriented for binding. The electrostatic potential (ranging from −433 kJ mol^{-1} to −105 kJ mol^{-1} in the (*S*) epimer, and from −433 kJ mol^{-1} to −99 kJ mol^{-1} in the (*R*) epimer) around the two epimers is quite different, as can be seen in Fig. 7, because the proximity of O_1 leads to a more negative region around the carbonyl oxygen (O_8) in the (*S*) epimer. This factor, and the unexpected disappearance of the minimum related to the carbonyl group in the (*R*) epimer, suggest that the biological properties of these epimers are quite different. These results agree with the prediction of Lamotte et al. [37] that the (*R*) epimer is unlikely to be active. Unfortunately, there are no experimental MIC values available for the pure epimers to confirm this prediction, which prevents lactivicin being used in the quantitative correlations. Of the whole set of inhibitor compounds, the (*S*) epimer shows the worst overlays, although it is probably responsible for the antibacterial activity. This is because the presence of O_1 significantly shifts the position of the minimum near the active carbonyl O_8. The poor electrostatic matching is consistent with the weak antibacterial activity shown by a mixture of both epimers.

TABLE 3
STRUCTURAL AND ELECTROSTATIC OVERLAYS OF TWO MODELS FOR THE SUBSTRATE AND LACTAM COMPOUNDS

Structure CSD ref.[d] MIC ($\mu g\,ml^{-1}$)[e] k_2/K ($M^{-1}\,s^{-1}$)[f]	Corresponding minima				Distance (Å)	Rms_{elec}[a] (Å)	Distances[b] (Å)	Rms_3_{atom} (Å)	$Rms_{struc/elec}$ (Å)	Rms_{struc}[c] (Å)
	Nearest inhibitor atom	V ($kJ\,mol^{-1}$)	Nearest substrate atom	V ($kJ\,mol^{-1}$)						
'Ampicillin' **1** Equatorial conformation of penicillin AMCILL 50.25 107	O_{14}	−331.7	O_1	−341.0 (−337.0)	0.34 (0.24)	0.44 (0.69)	1.12 (1.51) 0.83 (1.03) 0.50 (1.20)	0.86 (1.26)	0.75 (1.19)	0.52 (0.51)
	O_{10}/O_8	−485.6	O_3^A/O_2	−544.4 (−621.3)	0.66 (1.06)					
	O_{10}	−564.1	O_3^A	−612.8 (−627.3)	0.38 (0.82)					
	O_{11}	−573.7	O_3^B	−613.8 (−625.4)	0.31 (0.18)					
	(S_1)	−306.1	(N_3)	(−285.7)	(2.62)					
	(O_{14})	−331.7	(N_3)	(−285.7)	(3.58)					
'Penicillin V' **2** Axial conformation of penicillin JOTLAF	O_{14}	−359.0	O_1	−341.0 (−337.0)	0.64 (1.07)	1.36 (1.70)	1.09 (1.76) 0.38 (0.96) 0.60 (1.42)	0.75 (1.32)	1.76 (1.65)	0.83 (0.96)
	O_8	−378.6	O_3^A/O_2	−547.9 (−621.3)	2.21 (2.57)					
	O_{10}	−571.6	O_3^A	−612.8 (−627.3)	1.26 (1.33)					
	O_{11}	−600.0	O_3^B	−613.8 (−625.4)	0.73 (1.25)					
	O_{14}	−359.0	(N_3)	(−285.7)	(2.70)					
	O_{10}/S_1	−500.9	(N_3)	(−285.7)	(3.86)					
'Cephalotin' **3** CETHNA 8 3000	O_{15}	−325.4	O_1	−341.0 (−337.0)	0.19 (0.28)	0.47 (0.31)	0.81 (0.08) 0.74 (0.70) 1.11 (0.63)	0.90 (0.55)	1.33 (0.73)	0.44 (0.41)
	O_{11}/O_9	−616.8	O_3^A/O_2	−547.9 (−621.3)	0.72 (0.35)					
	O_{11}	−610.1	O_3^A	−612.8 (−627.3)	0.57 (0.30)					
	O_{12}	−597.1	O_3^B	−613.8 (−625.4)	0.11 (0.33)					
	(S_1)	−278.4	(N_3)	(−285.7)	(3.51)					
	(O_{15})	−325.4	(N_3)	(−285.7)	(3.51)					
Oxacephem **4** MOACPM 4.3	O_{15}/O_{17}	−411.2	O_1	−341.0 (−337.0)	0.54 (0.91)	0.49 (0.54)	0.54 (0.60) 0.50 (0.57) 1.14 (0.51)	0.78 (0.56)	1.46 (0.65)	0.52 (0.27)
	O_9/O_{11}	−559.6	O_3^A/O_2	−547.9 (−621.3)	0.55 (0.36)					
	O_{11}	−589.4	O_3^A	−612.8 (−627.3)	0.48 (0.36)					
	O_{12}	−584.8	O_3^B	−613.8 (−625.4)	0.35 (0.30)					
	O_{15}/O_1	−413.5	O_1	−341.0 (−337.0)	2.87 (3.00)					
	O_{17}/N_5	−337.3	O_1	−341.0	3.73					
	(O_{17}/N_5)	−337.3	(N_3)	(−285.7)	(2.70)					
	(O_{15}/O_1)	−413.5	(N_3)	(−285.7)	(2.70)					
	(O_{15}/O_{17})	−411.2	(N_3)	(−285.7)	(2.93)					

TABLE 3
(continued)

Structure CSD ref.[d] MIC ($\mu g\,ml^{-1}$)[e] k_2/K ($M^{-1}\,s^{-1}$)[f]	Corresponding minima				Distance (Å)	Rms_{elec} [a] (Å)	Distances[b] (Å)	Rms_3_{atom} (Å)	$Rms_{struc/elec}$ (Å)	Rms_{struc} [c] (Å)
	Nearest inhibitor atom	V ($kJ\,mol^{-1}$)	Nearest substrate atom	V ($kJ\,mol^{-1}$)						
Monobactam **5** PABJOR 66.7	O_{12}	−348.9	O_1	−341.0 (−337.0)	0.48 (0.91)	0.57[g] (0.89)	0.83 (1.39) 0.43 (0.78) 1.13 (1.53)	0.83 (1.29)	0.67 (1.26)	0.39 (0.44)
	O_4/O_9	−566.7	O_3^A/O_2	−547.9 (−621.3)	0.34 (0.41)					
	O_4	−542.2	O_3^A	−612.8 (−627.3)	0.80 (1.17)					
	O_{12}/Ph	−359.1	O_1	−341.0 (−337.0)	2.46 (2.20)					
	(O_{12})	(−348.9)	(N_3)	(−285.7)	(2.88)					
	O_4	−542.2	O_3^B	−613.8 (625.4)	1.81 (1.86)					
	O_3/O_4	−525.7	O_3^B	−613.8 (−625.4)	3.10 (2.76)					
	O_3/O_4	−526.2	O_3^B	−613.8 (−625.4)	2.92 (2.59)					
	O_3/O_4	−525.7	O_3^A	−612.8 (−627.3)	2.32 (2.92)					
	O_3/O_4	−526.2	O_3^A	−612.8 (−627.3)	2.11 (2.79)					
Imipenem **6** SAHSOJ 0.25 1000	O_{13}	−291.6	O_1	−341.0 (−337.0)	0.46 (0.08)	0.47 (0.24)	0.36 (0.75) 0.24 (0.47) 0.90 (0.61)	0.58 (0.62)	1.04 (0.81)	0.66 (0.63)
	O_{10}/O_8	−604.1	O_3^A/O_2	−547.9 (−621.3)	0.20 (0.35)					
	O_{10}	−617.3	O_3^A	−612.8 (−627.3)	0.70 (0.27)					
	O_{11}	−616.3	O_3^B	−613.8 (−625.4)	0.41 (0.15)					
	(O_{10}/N_4)	−566.4	(N_3)	(−285.7)	(3.54)					
Clavulanic acid **7** CLAVNT10 87.5 21	O_8	−370.3	O_3^A/O_2	−547.9 (−621.3)	1.96 (2.10)	1.39[g] (1.51)	1.25 (2.70) 0.59 (2.12) 0.87 (1.12)	0.94 (2.06)	1.13 (2.20)	0.68 (0.73)
	O_{10}	−571.6	O_3^A	−612.8 (−627.3)	1.13 (1.38)					
	O_{11}	−606.6	O_3^B	−613.8 (−625.4)	0.82 (0.72)					
	N_4/O_{10}	−519.6	O_3^A/O_2	−547.9 (−621.3)	2.61 (2.52)					
	C_2/C_{12}	−276.9	O_3^A/O_2	−547.9 (−621.3)	3.75 (3.82)					
	C_2–C_{12}	−276.9	(N_3)	(−285.7)	(1.30)					
Δ^2-cephem-4α-carboxylic acid **8** 128 68	O_{15}	−351.5	O_1	−341.0 (−337.0)	1.69 (2.24)	1.71 (2.11)	1.57 (1.97) 0.93 (1.53) 0.76 (1.48)	1.14 (1.67)	1.69 (1.73)	0.73 (0.95)
	O_9	−381.8	O_3^A/O_2	−547.9 (−621.3)	2.70 (3.09)					
	O_{11}	−564.4	O_3^A	−612.8 (−625.4)	0.93 (1.56)					
	O_{12}	−560.6	O_3^B	−613.8 (−625.4)	1.02 (1.26)					

TABLE 3
(continued)

Structure CSD ref.[d] MIC ($\mu g\,ml^{-1}$)[e] k_2/K ($M^{-1}\,s^{-1}$)[f]	Corresponding minima				Distance (Å)	Rms_{elec}[a] (Å)	Distances[b] (Å)	Rms_3_{atom} (Å)	$Rms_{struc/elec}$ (Å)	Rms_{struc}[c] (Å)
	Nearest inhibitor atom	V ($kJ\,mol^{-1}$)	Nearest substrate atom	V ($kJ\,mol^{-1}$)						
	O_{15}	−351.5	(N_3)	(−285.7)	(1.95)					
	O_{11}/S_1	−532.4	(N_3)	(−285.7)	(3.39)					
Δ^2-cephem-4β-carboxylic acid **9** 128	O_{15}	−353.8	O_1	−341.0 (−337.0)	0.40 (0.71)	0.96 (0.94)	1.37 (1.72) 1.65 (1.38) 3.04 (1.67)	2.15 (1.60)	2.90 (1.57)	1.17 (0.80)
	O_{11}/O_9	−607.6	O_3^A/O_2	−547.9 (−621.3)	0.79 (1.10)					
	O_{11}	−565.9	O_3^A	−612.8 (−627.3)	1.12 (0.94)					
	O_{12}	−558.7	O_3^B	−613.8 (−625.4)	1.28 (0.95)					
	S_1	−328.9	O_1	−341.0 (−337.0)	3.22 (3.40)					
	(S_1)	(−328.9)	(N_3)	(−285.7)	(2.68)					
	(O_{15})	(−353.8)	(N_3)	(−285.7)	(3.35)					
'Pyrazolidinone' **10** 1.67	O_{15}	−305.8	O_1	−341.0 (−337.0)	0.66 (0.26)	0.69 (0.21)	1.40 (0.68) 1.36 (0.76) 1.92 (0.56)	1.58 (0.67)	1.91 (0.69)	0.59 (0.41)
	O_{11}/O_9	−586.2	O_3^A/O_2	−547.9 (−621.3)	0.66 (0.22)					
	O_{11}	−566.6	O_3^A	−612.8 (−627.3)	0.96 (0.22)					
	O_{12}	−561.4	O_3^B	−613.8 (−625.4)	0.35 (0.12)					
	(N_4/N_5)	(−371.4)	(N_3)	(−285.7)	(2.96)					
γ-Azetidine **11** CUFJAO 100	O_{14}	−321.7	O_1	−341.0 (−337.0)	0.19 (0.38)	0.69 (1.01)	1.05 (1.79) 0.77 (1.07) 0.71 (1.13)	0.86 (1.35)	0.88 (1.33)	0.55 (0.57)
	O_8	−462.2	O_3^A/O_2	−547.9 (−621.3)	1.11 (1.50)					
	O_{10}	−589.8	O_3^A	−612.8 (−627.3)	0.72 (1.21)					
	O_{11}	−621.7	O_3^B	−613.8 (−625.4)	0.31 (0.25)					
	N_4/O_{10}	−551.2	O_3^A/O_2	−547.9 (−621.3)	2.54 (2.20)					
	(N_4/O_{10})	−551.2	(N_3)	(−285.7)	(3.74)					
	(O_{14})	−321.7	(N_3)	(−285.7)	(3.41)					
Lactivicin **12** (*S*) epimer FOJNAT	O_{14}	−312.7	O_1	−341.0 (−337.0)	0.53 (0.78)	0.98 (1.37)	1.44 (2.09) 1.01 (1.38) 0.74 (1.99)	1.10 (1.85)	1.37 (2.36)	0.40 (0.92)
	O_8/O_1	−548.7	O_3^A/O_2	−547.9 (−621.3)	1.59 (1.95)					
	O_{10}	−557.8	O_3^A	−612.8 (−627.3)	0.94 (1.73)					
	O_{11}	−557.4	O_3^B	−613.8 (−625.4)	0.42 (0.30)					
	O_{19}	−438.5	O_3^A/O_2	−547.9	3.82					
	(O_4)	(−524.7)	(N_3)	(−285.7)	(2.37)					
Lactivicin **13** (*R*) epimer	No minimum around the reactive carbonyl group could be detected and therefore it was not possible to get the electrostatic overlay									

TABLE 3
(continued)

Structure CSD ref.[d] MIC ($\mu g\ ml^{-1}$)[e] k_2/K ($M^{-1}\ s^{-1}$)[f]	Corresponding minima				Distance (Å)	Rms_{elec} [a] (Å)	Distances[b] (Å)	Rms_3_{atom} (Å)	$Rms_{struc/elec}$ (Å)	Rms_{struc} [c] (Å)
	Nearest inhibitor atom	V ($kJ\ mol^{-1}$)	Nearest substrate atom	V ($kJ\ mol^{-1}$)						
Deazacarbapenam **14** 128	O_8	−447.4	O_3^A/O_2	−547.9 (−621.3)	1.24 (1.39)	0.94[g] (1.10)	2.00 (3.10) 2.12 (3.58) 1.25 (1.78)	1.83 (2.92)	1.90 (3.26)	0.61 (0.63)
	O_{10}	−584.2	O_3^A	−612.8 (−627.3)	1.03 (1.30)					
	O_{11}	−585.6	O_3^B	−613.8 (−625.4)	0.21 (0.12)					

Overlay of the minima in the electrostatic potential 0.5 Å from the van der Waals surface of SAP and TS (in brackets) conformations of the substrate and β-lactam inhibitors (and other structures). The four minima that have been explicitly overlaid by minimising their rms separations are reported first, followed by all other pairs of minima within 4.0 Å of each other. The exact geometries were taken from the crystal structures, for which the Cambridge Structural Database [24] refcode is given in parentheses, with the hydrogen atoms added, to give N-H and C-H bond lengths of 1.01 Å and 1.08 Å, respectively [49].

[a] Rms_{elec} denotes the rms obtained in the electrostatic matching using the same four pair of minima.

[b] These are the distances obtained in the electrostatic matching between the O_2, C_2' and C_3' atoms and the corresponding atoms in the lactam structures. Rms_3_{atom} denotes the rms of these distances. $Rms_{struc/elec}$ is the rms obtained between all atoms included in overlay 3 for the geometry given by the electrostatic matching.

[c] Rms_{struct} is the rms obtained in the structurally optimised overlay 3 defined in Table 2.

[d] Crystal structure references: **1**, ampicillin [25]; **2**, penicillin V benzyl ester [50]; **3**, cephalotin sodium salt [26]; **4**, diphenylmethyl-7α-methoxy-3-(1-methyl-1*H*-tetrazol-5-yl-thio)-methyl-7β-phenylacetamido-1-oxa-1-dethia-ceph-3-em-4-carboxylate [51]; **5**, (3*S*,4*S*)-3-phenylacetamido-4-methyl-2-oxoazetidine-1-sulfonate [52]; **6**, imipenem [53]; **7**, (*Z*)-*p*-nitrobenzyl clavulanate [54]; **11**, γ-lactam azetidine [55]; **12**, 4-aminolactivinic acid [56].

[e] MIC has been defined as an average of the Minimum Inhibition Concentration of three gram-negative bacteria: *E. coli*, *K. pneumoniae* and *E. aerogenes*. MIC references: **1**, ampicillin and **3**, cephalotin [57]; **4**, oxacephem [58]; **5**, monobactam [59]; **6**, imipenem [45]; **7**, clavulanic acid [60]; **8**, Δ^2-cephem-4α-carboxylic acid and **9**, Δ^2-cephem-4β-carboxylic acid [6]; **10**, pyrazolidinone [61]; **11**, γ-lactam azetidine [62]; **12** and **13**, lactivicin [63]; **14**, deazacarbapenam [64].

[f] k_2/K references: **1**, ampicillin [65]; **3**, cephalotin and **8**, Δ^2-cephem-4α-carboxylic acid [5]; **6**, imipenem and **7**, clavulanic acid [66].

[g] Only three minima have been used to get the best electrostatic overlay.

Discussion

Two aspects of the molecular properties directly associated with antibacterial activity are the appropriate electrostatic and steric properties to be recognized as a transition-state analog of the natural D-alanyl-D-alanine substrate of the enzymes and the chemical reactivity of the lactam functionality. Focusing on the first requirement, only structural similarity has been used previously to try to distinguish between compounds with significant antibacterial activity and noninhibitors. Cohen [48] proposed that for biologically active compounds the distance between the carbon atom in the carboxylic function and the oxygen atom of the reactive carbonyl group would range from 3.0 Å to 3.9 Å. Lamotte et al. [37] proposed that the distance between the oxygen carbonyl in the lactam ring and in the side chain should range from 4.70 Å to 5.85 Å, and that the angle formed between the carbonyl oxygen atoms and the carbon atom in the carboxylic group should be in the range from 95° to 133°. These criteria provide a useful, but not infallible guide, since although most of the noninhibitor compounds studied in this work are outside these ranges, the *R* epimer of lactivicin (**13**) and the 7β(acetylamino)-Δ^2-cephem-4β-carboxylic acid (**9**) would wrongly be predicted to be active. In addition, ampicillin shows an $O_8\cdots C_9$ distance of 3.90 Å, which is exactly within Cohen's limit for active compounds, and yet it possesses a broad antibacterial spectrum. Our structural overlay analysis also demonstrates this moderate correlation, with the better overlays of the atoms of the two peptide groups and the carboxylate with corresponding atoms in the lactam compounds, generally being shown by the active inhibitor compounds. However,

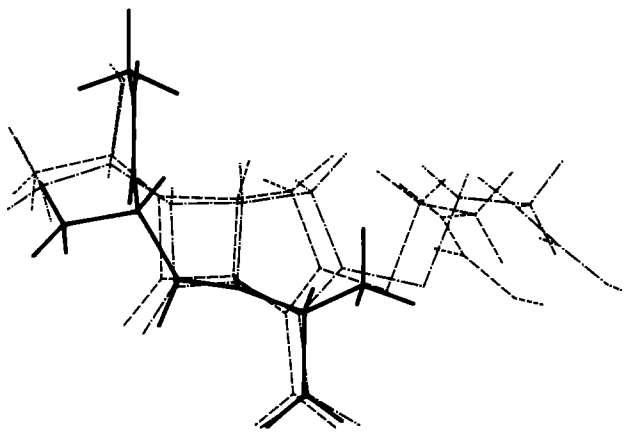

Fig. 8. Relative orientations of the strong inhibitor imipenem (**6**) in the electrostatic (–·–) and structural (–––) matching with the TS substrate (bold). The structural fitting is overlay 3, as defined in Table 2.

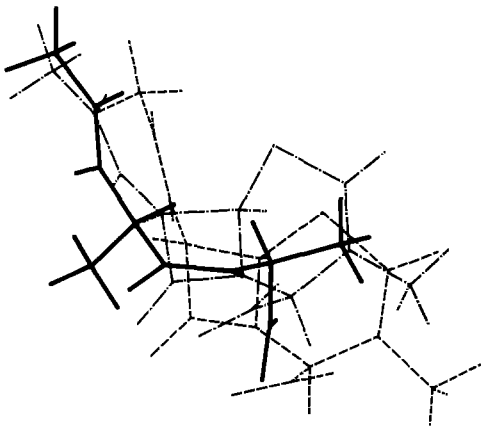

Fig. 9. Relative orientations of the poor inhibitor Δ^2-cephem-4β-carboxylic acid (**9**) in the electrostatic (–·–) and structural (–––) matching with the TS substrate (bold). The structural fitting is overlay 3, as defined in Table 2.

the noninhibitor compounds do not show sufficiently bad structural overlays for establishing a clear difference.

A first examination of the electrostatic potential around the charged substrate and possible inhibitors shows more marked similarities and differences. In both the substrate and the lactam compounds with antibacterial activity there is an area with a deep negative electrostatic potential close to the reactive region (Fig. 5). However, in compounds with little antibacterial activity, such as clavulanic acid, or noninhibitors, the electrostatic potential is rather different in this area (Fig. 6). The quantification of this observation shows that all inhibitor compounds and both models of the bound conformation of the substrate show two electrostatic minima related to the carboxylic group with a similar energy, another minimum between the reactive carbonyl group and the closest oxygen atom in the carboxylic group, and finally a minimum related to the oxygen atom on the 6/7 side chain. The relative disposition of the minima is different for the noninhibitors. In some cases (e.g. **2**), this results from a change in position of the carboxylate group, which makes the α-face of the ring more negative and the region around the reactive carbonyl group less negative (Fig. 6). By contrast, certain changes in functional groups, such as the substitution of a carboxylate by sulphonate in **5**, or replacement of a side-chain carbonyl group by a hydroxy group (**6**), can maintain the electrostatic similarity and, apparently, also the antibacterial activity.

The quality of the electrostatic matching can be crudely quantified by using the rms separations of the four minima of the substrate and the overlaid minima of the lactam compounds (rms_{elec}). A value of rms_{elec} that is significantly less than 1 Å is displayed by all the active and by none of the inactive compounds. The differentiation between inhibitors and noninhibitors is more marked if the minima are matched to those of the substrate model with a pyramidal nitrogen (TS).

Although the overlay of electrostatic rather than structural features gives a better differentiation of antibacterial activity, the two properties are closely linked. Figure 8 shows the relative orientation of a good inhibitor (imipenem, **6**) and the substrate (TS), as predicted by either overlaying the electrostatic minima or by optimising the structural overlay. Both orientations are very similar. By contrast, for the noninhibitor 7β(acetylamino)-Δ^2-cephem-4β-carboxylic acid (**9**), the two overlay methods produce markedly different orientations of the lactam compound (Fig. 9).

Hence, included in Table 3 are the rms separations of the atoms O_2, C_2' and C_3' to the equivalent atoms of the lactam structures for the relative orientation defined by the electrostatic matching (rms_3_{atom}). The rms values for

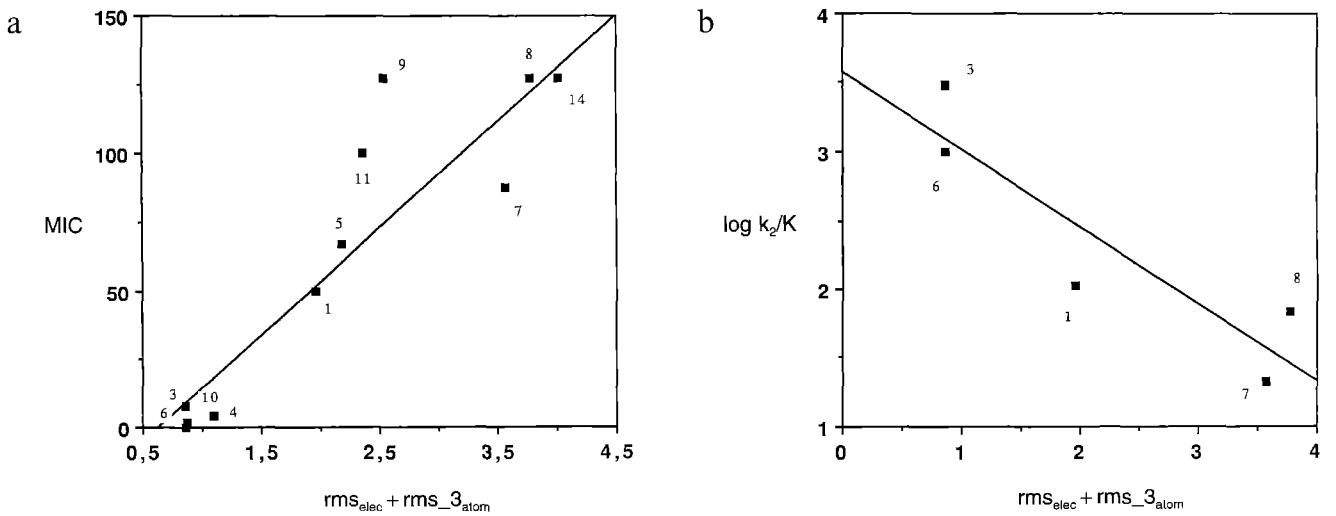

Fig. 10. (a) Correlation between the average MIC (Minimum Concentration for Inhibition) for a set of gram-negative bacteria (*Escherichia coli*, *Klebsiella pneumoniae* and *Enterobacter aerogenes*) and a combination of electrostatic and structural overlays, as defined in Table 3, rms_{elec} + rms_3_{atom}, obtained with substrate model TS. (b) Correlation between the log (k_2/K) for DD-peptidase R61 and a combination of electrostatic and structural overlays, as defined in Table 3, rms_{elec} + rms_3_{atom}, obtained with substrate model TS.

the extended overlay ($rms_{struc/elec}$) are also given. Both of these measures show a good structural overlay for all the inhibitors, and therefore either electrostatic or structural matching predicts a similar relative orientation of the inhibitor to the substrate.

The average steric and electrostatic overlay measure in the electrostatic overlay orientation provides a better correlation with the average of the MIC of three gram-negative bacteria: *E. coli*, *K. pneumoniae* and *E. aerogenes* (Fig. 10a) ($MIC = -25.557 + 40.818\ (rms_{elec} + rms\_3_{atom})$, $r^2 = 0.830$). This electrostatic/structural parameter has also been correlated with the available kinetic data for the inhibition of the serine peptidase of *Streptomyces* R61. A plot of log k_2/K, the ratio of the first-order rate constant of acylation to the dissociation constant, as defined by Frere et al. [5] ($\log k_2/K = 3.575 - 0.564\ (rms_{elec} + rms\_3_{atom})$, $r^2 = 0.819$), is shown in Fig. 10b. These are quite acceptable correlations, given the crudity of these measures of the electrostatic and structural similarity, as well as the variation in inhibitory values for different bacteria. As can be seen, those compounds with an adequate chemical reactivity show a strong correlation between the steric/electrostatic parameter and the antibacterial or kinetic parameters. Deviations of this behaviour may also be related to a reduced chemical reactivity or an inadequate electronic structure that does not allow delocalization in the process of expulsion of the group at position 2 or 3.

Conclusions

The structural and electrostatic properties analysis of a set of representative β-lactam, γ-lactam and nonlactam structures shows that all strong inhibitors of the DD-peptidase enzymes have four minima that can be placed within 1 Å of the equivalent minima of the substrate, in a sterically plausible relative orientation. These overlays produce an overall match of the electrostatic and steric properties, consistent with the inhibitor binding to the enzyme within the same site as D-alanyl-D-alanine. The electrostatic matching provides a better correlation with antibacterial activity than the structural matching and previous structure-based predictive criteria. However, both features cannot be considered independently. The best discrimination between inhibitor and noninhibitor compounds is a semiquantitative correlation using the experimental minimum concentration for inhibition and parameters describing the separation of both minima and atoms in the relative orientations predicted by the electrostatic overlay.

The apparent importance of the relative orientations of the electrostatic minima in determining antibacterial activity can partly be rationalised by assuming that the matched extrema are close to polar binding groups of the opposite sign in the binding site. On the other hand, the electrostatic pattern around all the noninhibitor structures is so different from that of the substrate, that the binding of these compounds in the active site would be unfavourable.

We have found a combination of electrostatic and structural properties of reactive lactams that can differentiate semiquantitatively between inhibitors and non-inhibitors of DD-peptidase enzymes. This methodology, which does not require a detailed knowledge of enzyme structure, should be helpful in designing new inhibitors, though we must keep in mind that these are not the only parameters that determine the antibacterial properties of β-lactam compounds and chemical reactivity. The diffusion rate through the outer membrane of bacteria also affects antibacterial activity. More direct predictions of potential antibiotic recognition should be possible when accurate structures of the carboxy- and transpeptidase enzyme binding sites can be established. Such modelling should eventually give us a more detailed understanding of the inhibition process, and hence rationalise our observations.

Acknowledgements

J.F. thanks the European Commission, Human Capital and Mobility Scheme, for a Research Fellowship (EBR4001GT931410). The computing equipment was provided under an EPSRC grant (GR/J31865). We would like to thank Dr. J.G. Vinter and Dr. T. Mitchell for constructive comments. J.F. thanks R.P. Apaya for his help in the use of the ORIENT program, the construction of the colour figures and his continual support.

References

1 Georgopapadakou, N.H. and Sykes, R.B., Handb. Exp. Pharmacol., 67 (1983) 1.
2 Waxman, D.J. and Strominger, J.L., Annu. Rev. Biochem., 52 (1983) 825.
3 Tipper, D.J. and Strominger, J.L., Proc. Natl. Acad. Sci. USA, 54 (1965) 75.
4 Lee, B., J. Mol. Biol., 61 (1971) 463.
5 Frere, J.M., Kelly, J.A., Klein, D., Ghuysen, J.M., Claes, P. and Vanderhaeghe, H., Biochem. J., 203 (1982) 223.
6 Cohen, N.C., Ernest, I., Fritz, H., Fuhrer, H., Rihs, G., Scartazzini, R. and Wirz, P., Helv. Chim. Acta, 70 (1987) 1967.
7 Wolfe, S. and Hoz, T., Can. J. Chem., 72 (1994) 1044.
8 Rodriguez, J., Manaut, F. and Sanz, F., J. Comput. Chem., 14 (1993) 922.
9 Weinstein, H. and Osman, R., In Richards, W.G. (Ed.) Computer-Aided Molecular Design, IBC Technical Services, London, U.K., 1989, pp. 105–118.
10 Richards, N.G.J. and Vinter, J.G., J. Comput.-Aided Mol. Design, 5 (1991) 1.
11 Orozco, M., Canela, E.I. and Franco, R., Mol. Pharmacol., 35 (1989) 257.
12 Van de Waterbeemd, H., Carrupt, P.A. and Testa, B., J. Med. Chem., 29 (1986) 600.

13 Luque, F.J., Sanz, F., Illas, F., Pouplana, R. and Smeyers, Y.G., Eur. J. Med. Chem., 23 (1988) 7.
14 Martin, M., Sanz, F., Campillo, M., Pardo, L., Perez, J. and Turmo, J., Int. J. Quantum Chem., 23 (1983) 1627.
15 Manaut, F., Lozoya, E. and Sanz, F., In Silipo, C. and Vitoria, A. (Eds.) QSAR: Rational Approaches to the Design of Bioactive Compounds, Elsevier, Amsterdam, the Netherlands, 1991, pp. 339–342.
16 Davis, A., Warrington, B.H. and Vinter, J.G., J. Comput.-Aided Mol. Design, 1 (1987) 97.
17 Vinter, J.G. and Trollope, K.I., J. Comput.-Aided Mol. Design, 9 (1995) 297.
18 Stone, A.J. and Alderton, M., Mol. Phys., 56 (1985) 1047.
19 Apaya, R.P., Lucchese, B., Price, S.L. and Vinter, J.G., J. Comput.-Aided Mol. Design, 9 (1995) 33.
20 Van der Wenden, E.M., Price, S.L., Apaya, R.P., IJzerman, A.P. and Soudijn, W., J. Comput.-Aided Mol. Design, 9 (1995) 44.
21 Labischinski, H., Barnickel, G., Naumann, D., Ronspeck, W. and Bradaczek, H., Biopolymers, 24 (1985) 2087.
22 Dauber-Osguthorpe, P., Roberts, V.A., Osguthorpe, D.J., Wolff, J., Genest, M. and Hagler, A.T., Protein Struct. Funct. Genet., 4 (1988) 31.
23 Insight II User Guide, v. 2.3.0, Biosym Technologies, San Diego, CA, 1993.
24 Allen, F.H., Davies, J.E., Galloy, J.J., Johnson, O., Kennard, O., Macrae, C.F., Mitchell, E.M., Mitchell, G.F., Smith, J.M. and Watson, D.G., J. Chem. Inf. Comput. Sci., 31 (1991) 187.
25 Boles, M.O. and Girven, R.J., Acta Crystallogr., B32 (1976) 2279.
26 Van Meerssche, M., Germain, G., Declercq, J.P., Coene, B. and Moreaux, C., Cryst. Struct. Commun., 8 (1979) 287.
27 De Coen, J.L., Lamotte-Brasseur, J., Ghuysen, J.M., Frere, J.M. and Perkins, H.R., Eur. J. Biochem., 121 (1981) 221.
28 Virudachalam, R. and Rao, V.S.R., Int. J. Pept. Protein Res., 10 (1977) 51.
29 Neuhaus, F.C. and Hammes, W.P., Pharmacol. Ther., 14 (1981) 265.
30 Simon, G.L., Morin, R.B. and Dahl, L.F., J. Am. Chem. Soc., 94 (1972) 8557.
31 Kelly, J.A., Knox, J.R., Zhao, H., Frere, J.M. and Ghuysen, J.M., J. Mol. Biol., 209 (1989) 281.
32 Boyd, D.B., J. Chem. Ed., 53 (1976) 483.
33 Boyd, D.B., J. Med. Chem., 18 (1975) 408.
34 Laws, A.P. and Page, M.I., J. Chem. Soc., Perkin Trans. 2, (1989) 1577.
35 Rao, V.S.R. and Vasudevan, T.K., CRC Crit. Rev. Biochem., 14 (1983) 173.
36 Blanpain, P.C., Nagy, J.B., Laurent, G.H. and Durant, F.V., J. Med. Chem., 23 (1980) 1283.
37 Lamotte, J., Dive, G. and Ghuysen, J.M., Eur. J. Med. Chem., 26 (1991) 43.
38 Binkley, J.S., Pople, J.A. and Hehre, W.J., J. Am. Chem. Soc., 102 (1980) 939.
39 CADPAC5: The Cambridge Analytical Derivatives Package, Issue 5.0, 1992. A suite of quantum chemistry programs developed by Amos, R.D., with contributions from Alberts, I.L., Andrews, J.S., Colwell, S.M., Handy, N.C., Jayatilaka, D., Knowles, P.J., Kobayashi, R., Koga, N., Laidig, K.E., Malsen, P.E., Murray, C.W., Rice, J.E., Sanz, J., Simandiras, D., Stone, A.J. and Su, M.D.
40 Price, S.L., Andrews, J.S., Murray, C.W. and Amos, R.D., J. Am. Chem. Soc., 114 (1992) 8268.
41 a. Price, S.L. and Stone, A.J., J. Chem. Phys., 86 (1987) 2859.
b. Stone, A.J., ORIENT v. 2: A program for calculating the electrostatic interactions between molecules, University of Cambridge, Cambridge, U.K., 1990.
42 Boyd, D.B., J. Med. Chem., 27 (1984) 63.
43 Boyd, D.B., Eigenbrot, C., Indelicato, J.M., Miller, J.M., Pasini, C.E. and Woulfe, S.R., J. Med. Chem., 30 (1987) 528.
44 Boyd, D.B., Snoddy, J.D. and Lin, H.-S., J. Comput. Chem., 12 (1991) 635.
45 Page, M.I. (Ed.) The Chemistry of β-Lactams, Chapman and Hall, New York, NY, 1992.
46 Goodman Gilman, A. and Goodman, L.S. (Eds.) The Pharmacological Basis of Therapeutics, Editorial Medica Panamericana, Buenos Aires, Argentina, 1986.
47 Baldwin, J.E., Lynch, G.P. and Pitlik, J., J. Antibiot., 44 (1991) 1.
48 Cohen, N.C., J. Med. Chem., 26 (1983) 259.
49 Allen, F.H., Kennard, O., Watson, D.G., Brammer, L., Orpen, A.G. and Taylor, R., J. Chem. Soc., Perkin Trans. 2, S1 (1987).
50 Shin, W. and Woo Cho, S., Acta Crystallogr., C48 (1992) 1447.
51 Shiro, M., Nakai, H., Onoue, H. and Narisada, M., Acta Crystallogr., B36 (1980) 3137.
52 Balsamo, A., Domiano, F., Macchia, B., Macchia, F. and Rossello, A., Eur. J. Med. Chem., Chim. Ther., 26 (1991) 339.
53 Ratcliffe, R.W., Wildonger, K.J., di Michele, L., Douglas, A.W., Hajdu, R., Goegelman, R.T., Springer, J.P. and Hirshfield, J., J. Org. Chem., 54 (1989) 653.
54 Brown, A.G., Corbett, D.F., Goodacre, J., Harbridge, J.B., Howarth, T.T., Ponsford, R.J., Stirling, I. and King, T.J., J. Chem. Soc., Perkin Trans. 1, (1984) 635.
55 Baldwin, J.E., Adlington, R.M., Jones, R.H., Schofield, C.J., Zaracostas, C. and Greengrass, C.W., J. Chem. Soc., Chem. Commun., (1985) 194.
56 Wada, Y., Takamoto, M., Tsubotani, S. and Kamiya, K., Acta Crystallogr., C43 (1987) 1786.
57 Pearlman, D. (Ed.) Structure–Activity Relationships among the Semisynthetic Antibiotics, Academic Press, New York, NY, 1977.
58 Morin, R. and Gorman, M. (Eds.) Chemistry and Biology of β-Lactam Antibiotics: Nontraditional β-Lactam Antibiotics, Vol. 2, 1982.
59 Morin, R. and Gorman, M. (Eds.) Chemistry and Biology of β-Lactam antibiotics: Biochemistry, Vol. 3, 1982.
60 Demain, A.L. and Solomon, N.A. (Eds.) Antibiotics Containing the β-Lactam Structure II, Springer, Berlin, Germany, 1983.
61 Ternansky, R.J. and Draheim, S.E., J. Med. Chem., 36 (1993) 3119.
62 Baldwin, J.E., Adlington, R.M., Jones, R.H., Schofield, C.J., Zaracostas, C. and Greengrass, C.W., Tetrahedron, 17 (1986) 4879.
63 Nozaki, Y., Katayama, N., Ono, H., Tsubotani, S., Harada, S., Okazaki, H. and Nakao, Y., Nature, 325 (1987) 179.
64 Gordon, E.M., Pluscec, J. and Ondetti, M.A., Tetrahedron Lett., 22 (1981) 1871.
65 Frere, J.M., Biochem. Pharmacol., 26 (1977) 2203.
66 Kelly, J.A., Frere, J.M., Klein, D. and Ghuysen, J.M., Biochem. J., 199 (1981) 129.